Theoretical Study of Ring Exchange in the Borocenium Cation, $[B(C_5R_5)_2]^+$ (R = H, Me)

Ohyun Kwon and Michael L. McKee*

Department of Chemistry, Auburn University, Auburn, Alabama 36849

Received: June 19, 2001; In Final Form: September 6, 2001

Geometries and energetics of the borocenium cation, $[BCp_2]^+$, and the decamethylborocenium cation, $[BCp^*_2]^+$, have been studied by using density functional theory (DFT) and ONIOM methods. Possible structures with different hapticities were considered for $[BCp_2]^+$ at the B3LYP/6-31+G(d) level, and for $[BCp^*_2]^+$ at the ONIOM(B3LYP/6-31+G(d):HF/STO-3G) level. In the ground-state structure of $[BCp^*_2]^+$ one ring is monohapto and one ring is pentahapto (η^1/η^5), in good agreement with experiment. The energy difference between the η^1/η^5 (**A**) and η^5/η^5 (**I**) structure of $[BCp_2]^+$ is 54.5 kcal/mol at the B3LYP/6-311+G(2d,p)// B3LYP/6-31+G(d)+ZPC level, which is in contrast to the small energy difference (∼2 kcal/mol) found between the η^1/η^5 and η^5/η^5 structures in the isoelectronic Cp_2Be system. The ring exchange process for the $[BCp_2]^+$ cation has an activation energy barrier of 14.7 kcal/mol where the hapticity of one ring gradually decreases ($\eta^5 \rightarrow \eta^2$(TS) $\rightarrow \eta^2 \rightarrow \eta^1$(TS) $\rightarrow \eta^1$) and the hapticity for the other ring gradually increases ($\eta^1 \rightarrow \eta^1(TS)\rightarrow \eta^2 \rightarrow \eta^2$(TS) $\rightarrow \eta^5$). GIAO/B3LYP/6-31+G(d,p) calculations for the $[BCp^*_2]^+$ ^{11}B and ^{13}C chemical shifts are in excellent agreement with experiment. The decamethyl-substituted Cp donates more electron density to boron compared to Cp resulting in a 5.4 ppm downfield ^{11}B chemical shift for $[BCp^*_2]^+$ relative to $[BCp_2]^+$.

Introduction

The cyclopentadienyl (C_5H_5 = Cp) ligand has played a major role in the development of organometallic chemistry since the structure of ferrocene (Cp_2Fe) was identified in 1952,[1] and much effort in experiment and theory has focused on metallocenes of transition metals as well as main group elements. Over the past decade, main group metallocenes have attracted the attention of chemists[2] because of their structural fluxionality and synthetic utility as precursors for the chemical vapor deposition (CVD) process[3] in organometallic chemistry. In main group metallocenes, the broad range of electronegativities of main group elements (E) leads to either ionic or covalent bonding for Cp−E interactions. In contrast to the metallocenes of transition metals, π-type interactions between main group elements (E) and cyclopentadienyl (Cp) rings become weaker due to the absence of d-orbitals resulting in deviations from typical parallel sandwich structures.

Beryllocene (Cp_2Be) is a well-known example of a slip-sandwich η^1/η^5 structure in the solid[4] and gas phases[5] as well as many theoretical works.[6] A singlet ^{1}H NMR spectrum at −135 °C indicates that beryllocene in solution is highly fluxional due to the fast change of ring hapticities.[7] Blöchl and co-workers carried out dynamics calculations on beryllocene and found that the fluxional rearrangement occurs from an η^1/η^5 ground state over η^2/η^5 and η^3/η^3 transition states with small activation energy barriers (1.2 and 1.9 kcal/mol, respectively).[6m−6o] The symmetric η^5/η^5 structure (D_{5h} symmetry) is 2.2 kcal/mol higher than the ground state.[6m−6o]

Metallocene cations of Group 13 elements are isoelectronic with the corresponding neutral metallocenes of Group 2 elements. Experimentally known Group 13 metallocenes include decamethylborocenium cation, $[BCp^*_2]^+$ ($Cp^* = C_5Me_5$),[8] decamethylaluminocenium cation, $[AlCp^*_2]^+$,[9] and decamethylgallocenium cation, $[GaCp^*_2]^+$.[10] It is interesting to note that the structural behavior of these three group 13 metallocenes are quite different from each other. For instance, the $[BCp^*_2]^+$ and $[GaCp^*_2]^+$ cations were characterized as an η^1/η^5 slip-sandwich structure in the solid state by Cowley and co-workers[8b,10] while the $[AlCp^*_2]^+$ cation has a D_{5d}-symmetry structure in the crystal.[9] In addition, the borocenium cation might be a good catalyst for olefin polymerization since $[AlCp_2]^+$ of Group 13 metallocene has been shown to be an effective initiator for the polymerization of isobutene.[11]

In the present work, density functional theory (DFT)[12] calculations are applied to possible conformers of the borocenium cation, $[BCp_2]^+$, to investigate geometries and the lowest energy pathway for exchange among different hapticities. The sterically bulky pentamethylcyclopentadienyl (Cp*) ligand has successfully been used to synthesize monomeric forms of metallocenes, and structure of the $[BCp^*_2]^+$ cation has recently been determined in the solid.[8b] The nature of bonding between Cp* and a metal is anticipated to be similar to that of Cp, but Cp* is more sterically bulky, more electron-dative, and more "organic" than Cp.[13] To investigate the influence of Cp* rings on the structure and electronic properties of borocenium cations, a theoretical study is made using the combined QM/QM approach.[14]

Computational Details

Geometries of possible structures of the parent borocenium cation, $[BCp_2]^+$, were optimized[15] at the B3LYP/6-31+G(d) level[16] within the indicated symmetry constraint. Vibrational frequencies were calculated in order to determine the nature of the stationary points on the potential energy surface. Single-point calculations were performed on the optimized geometries of $[BCp_2]^+$ at the B3LYP/6-311+G(2d,p) level. The two-layered QM/QM ONIOM(B3LYP/6-31+G(d):HF/STO-3G) method[17] was employed to optimize the geometries of the bulky decamethyl-substituted borocenium cation. The real system, the complete $[BCp^*_2]^+$ cation, is treated at the HF/STO-3G level to model methyl group substituent effects, while the model system, the parent $[BCp_2]^+$ cation, is described at the B3LYP/

10.1021/jp012345p CCC: $20.00
Published on Web 10/16/2001

TABLE 1: Relative Energies (kcal/mol) of $[BCp_2]^+$ at Various Theoretical Levels

species	P. G.	type	NIF[a]	B3LYP /6-31+G(d)	B3LYP /6-31+G(d) +ZPC	B3LYP /6-311+G(2d,p) +ZPC[b,c]	MP2 /6-31+G(d) +ZPC[b,c]	MP4 /6-31+G(d) +ZPC[b,c]	CCSD(T) /6-31+G(d) +ZPC[b,c]
A	C_s	η^1/η^5	0	0.0	0.0	0.0	0.0	0.0	0.0
B	C_s	η^1/η^5	0	0.1	0.2	0.1			
C	C_2	η^2/η^2	0	15.7	14.2	13.5	20.2	18.9	20.4
D	C_1	η^1/η^2	1	17.4	15.7	14.7	21.0	20.0	21.1
E	C_{2h}	η^1/η^1	2	23.4	21.1	19.4			
F	C_s	η^2/η^5	2	23.7	22.5	23.0			
G	C_{2v}	η^1/η^1	2	32.0	29.5	26.9			
H	C_{2v}	η^2/η^2	4	43.7	40.6	39.4			
I	D_{5d}	η^5/η^5	4	56.1	53.7	54.5			
J	D_{5h}	η^5/η^5	5	56.7	54.5	55.3			

[a] Number of imaginary frequencies at the B3LYP/6-31+G(d) level. [b] Based on optimized geometries at the B3LYP/6-31+G(d) level. [c] ZPC from vibrational frequency calculations at B3LYP/6-31+G(d) level.

6-31+G(d) level. It has been shown that the integrated MO/MO approach (ONIOM) provides a reasonable description for larger systems which would otherwise require extensive computer resources.[17,18] Geometry optimizations of some conformers (**AA**, **BB**, and **CC**, see Figure 4)[19] of $[BCp^*_2]^+$ cations were also performed at the full B3LYP/6-31+G(d) level. The comparison between ONIOM and full DFT optimized geometries was satisfactory. Unless otherwise noted, relative energies of $[BCp_2]^+$ structures will be at the B3LYP/6-311+G(2d,p)//B3LYP/6-31+G(d)+ZPC level, whereas relative energies of $[BCp^*_2]^+$ structures will be at the B3LYP/6-31+G(d)//ONIOM-(B3LYP/6-31+G(d):HF/STO-3G) level (without zero-point corrections). Calculations for $[BCp^*_2]^+$ structures were also made at ONIOM(B3LYP/6-311+G(2d,p):HF/STO-3G)//ONIOM-(B3LYP/6-31+G(d):HF/STO-3G), but it was judged that the effect of steric repulsion was somewhat exaggerated at that level of theory.

Natural bond orbital (NBO)[20] analysis (including Wiberg Bond Indices (WBI)[21]) was used to compute atomic charges and bond orders for both $[BCp_2]^+$ and $[BCp^*_2]^+$ cations at the B3LYP/6-31+G(d) level. Chemical shifts were computed by using the GIAO method[22] with several basis sets. All calculated ^{11}B shielding values were referenced to B_2H_6 as the primary reference point. The resulting chemical shifts were converted to the standard $BF_3{\cdot}Et_2O$ scale using the experimental value of +16.6 ppm for δ (B_2H_6),[23] i.e., $\delta(^{11}B) = \sigma(^{11}B \text{ of } B_2H_6) - \sigma(^{11}B) + 16.6$. Calculated ^{13}C chemical shifts were referenced to the calculated absolute shielding of TMS ($SiMe_4$).

Results and Discussions

$[BCp_2]^+$ Structures. Optimized geometries of $[BCp_2]^+$ cations at the B3LYP/6-31+G(d) level are shown in Figure 1, and computed relative energies are given in Table 1. The lowest energy structure (**A**) of the $[BCp_2]^+$ cation has an eclipsed η^1/η^5 type C_s-symmetry structure (i.e., each Cp ring is eclipsed with respect to the B−C(σ) bond). Conformer **B** also has an η^1/η^5 type geometry but has a staggered orientation. **A** and **B** are both minima with an energy difference of only 0.1 kcal/mol at the standard level, which suggests that there is free rotation of the η^5-Cp ring. It is noted that the computed angle between the B−C(σ) bond and the least-squares plane of the η^1-Cp ring for **A** and **B** are 119.0° and 119.1°, respectively, in reasonable agreement with the experimental value for the $[BCp^*_2]^+$ cation (114.4°)[8b] as well as comparable with the DFT-optimized geometry (106.2°) of Cp_2Be,[24] which is isoelectronic with $[BCp_2]^+$. The pattern of distances of B−C and C−C bonds of the η^1-Cp ring and η^5-Cp ring are quite different. The B−C(σ) bond distance (1.568 Å) in η^1-Cp ring is much shorter than the

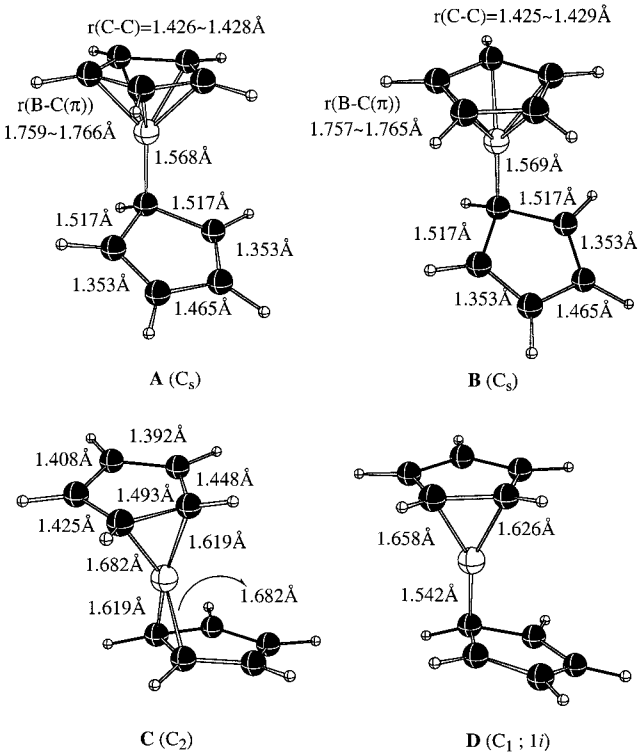

Figure 1. Optimized geometries of $[BCp_2]^+$ at B3LYP/6-31+G(d) level.

five other B−C(π) bond distances (1.759 ∼ 1.766 Å) in η^5-Cp ring for both **A** and **B**. The Wiberg Bond Index (WBI),[21] a computational measure of bond order, indicates that the B−C(σ) bond is a typical single bond (WBI = 0.93). Computed C−C bond distances in the η^5-Cp ring are in the range of 1.425 ∼ 1.429 Å for both **A** and **B**, whereas C−C distances in η^1-Cp ring shows alternating single-bond and double-bond characters (see Figure 1). Thus, the geometry of the η^5-Cp ring exhibits typical aromatic character with electron delocalization, whereas the geometry of η^1-Cp ring is dominated by the C−C bond alternation of a diene. Indeed, the localization of η^1-Cp ring with sp^3 hybridization of the C(σ) bonded to boron leads to improve the σ-bonding ability of η^1-Cp ligand, while the aromatic η^5-Cp ring contributes five π electrons to bonding. Using typical electron counting rules, the electron count around boron in the η^1/η^5 structure (**A** and **B**) is eight, i.e., the octet rule is satisfied.

C is a C_2-symmetry structure and characterized as a minimum (13.5 kcal/mol less stable in energy than **A**) where the Cp rings are coordinated to the boron in an η^2/η^2 bonding style. This η^2

bonding is confirmed by the fact that two B−C bond distances of 1.619 Å (WBI = 0.69) and 1.682 Å (WBI = 0.59) are significantly shorter than the other three B−C distances (2.444, 2.486, and 2.860 Å) for each Cp ring. On the other hand, the η^2 B−C bond distances are longer than the B−C(σ) single bond distance in **A** and **B** (1.568, 1.569 Å). Two η^2-Cp rings are identical with respect to the C_2 axis and the C−C bond distances in the Cp rings are in the range of 1.392 ∼ 1.493 Å, which implies that η^2-Cp ring is more localized than the η^5-Cp ring.

D is characterized as a transition structure, where one Cp ring is bonded to the boron as η^1 and the other Cp ring as η^2. The two B−C bond distances in η^2 style are computed to be 1.626 Å (WBI = 0.64) and 1.658 Å (WBI = 0.59), which are almost the same as those of **C**. However, the other three B−C distances (2.232, 2.563, 2.260 Å) become shorter than those of **C**, which indicates that the boron atom is closer to the ring centroid of Cp than in **C**. The distance of boron and the η^1-Cp ring is 1.542 Å (WBI = 0.87) which is slightly shorter than the corresponding distance in **A** and **B**. The transition vector (imaginary frequency), animated by Molden program,[25] clearly indicates that **D** connects **A** and **C** (**A** → **D(TS)** → **C**). The computed activation barrier for ring exchange process was 14.7 kcal/mol at the standard level and 21.1 kcal/mol at the CCSD(T)/6-31+G(d)//B3LYP/6-31+G(d)+ZPC level.

E, with η^1/η^1 type Cp rings (C_{2h}-symmetry), is 19.4 kcal/mol higher than **A** and characterized by two imaginary frequencies. The B−C bond distance is computed to be 1.525 Å (WBI = 0.85) showing single-bond character. It is noted that two Cp rings are parallel (∠Cp−Cp = 0.0°) and *trans*-oriented (see Figure 1). **F** has an η^2/η^5 type structure (2 imaginary frequencies) where the B−C bonds (1.767 Å; WBI = 0.56) involving the η^2 ring is somewhat longer than in **C** and **D**. For the η^5-Cp ring in **F**, the five B−C(π) bond distances (1.793 ∼ 1.845 Å) are similar to those in **A** and **B**, with C−C bond distances in the range of 1.420 ∼ 1.432 Å, indicating a delocalized Cp ring. The geometry of **G** is similar to that of **E**, but the two Cp rings are *cis*-oriented relative to each other, which results in nonparallel Cp rings (∠Cp−Cp = 38.0°) due to steric hindrance. **H** has an η^2/η^2 type geometry where the two B−C bonds are 1.689 Å (WBI = 0.58). **C** and **H** are both η^2/η^2 structures but **H** is less stable than **C** by 25.9 kcal/mol because the two Cp rings in **H** are *cis*-oriented resulting in more steric repulsion, whereas the orientations of Cp rings in **C** are shifted to avoid steric hindrance. **I** and **J** are both parallel sandwich complexes (D_{5d} and D_{5h} symmetries) with 4 and 5 imaginary frequencies, respectively.[8b] The C−C bond distances in **I** and **J** are 1.421 Å, whereas the B−C(π) distances are 1.942 and 1.946 Å, respectively, somewhat longer than those of **A**, **B**, and **F**, but comparable with the corresponding distances in the D_{5d} and D_{5h} structures of beryllocene[24c] (2.055 and 2.057 Å, respectively). The η^5/η^5 structures of **I** and **J** are higher in energy than **A** by 54.5 and 55.3 kcal/mol, respectively. Previous work by Marynick and co-workers[6p] on Cp_2Be (isoelectronic with $[BCp_2]^+$) predicted that the computed energy difference between the D_{5d} and C_s structures (the lowest conformer of Cp_2Be) was 4.3 kcal/mol at the B3LYP/6-311G(d,p)//B3LYP/6-31G(d) level. It is interesting to note that the $\eta^1/\eta^5-\eta^5/\eta^5$ energy separation is quite different in Cp_2Be and $[BCp_2]^+$. This may be due to the smaller covalent radius of the boron atom compared to the beryllium atom (0.90 and 1.25 Å, respectively[26]) resulting in more repulsion between both Cp rings in η^5/η^5 type of borocenium. Alternatively, the much more contracted p-orbitals of boron in $[BCp_2]^+$ compared to the p-orbitals of beryllium in Cp_2Be (due to the greater positive charge on the boron) would lead to much less overlap between the metal and the rings in $[BCp_2]^+$ relative to Cp_2Be. Thus, both effects lead to less stability of the parallel sandwich structure.[2e] It is also noted that the ring−ring distance for **I** (D_{5d} structure) is 3.040 Å, much smaller than that found in the D_{5d} structure of Cp_2Be (3.325 Å).[24]

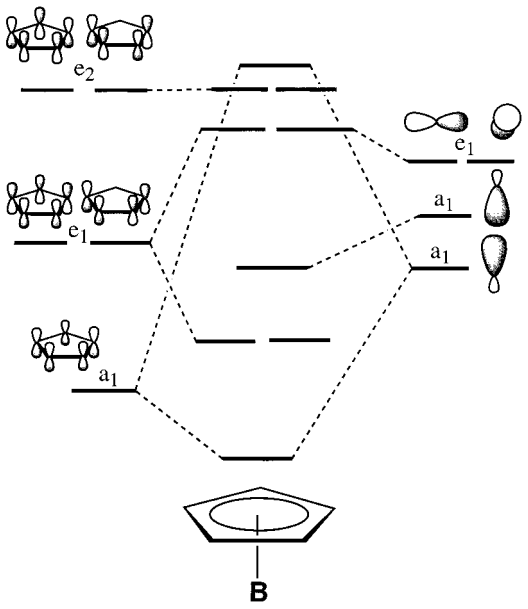

Figure 2. Molecular orbital diagram for BCp.

A molecular orbital interaction diagram of the atomic orbitals of boron with the symmetry-adapted group orbitals of one Cp ring is shown in Figure 2. The overlap between the degenerate p_x and p_y orbitals of the boron and the e_1 orbitals of the Cp ring leads to π-type bonding orbitals (e_1) which are the primary orbital interactions between boron and the Cp ring. However, the smaller p_x and p_y orbitals of boron cannot overlap as effectively with the e_1 orbitals of both Cp rings as is possible for a larger main group or transition metal atom. The result is a more stable η^1/η^5 structure compared to an η^5/η^5 structure. The smaller size of the boron atom also leads to hydrogen atoms of the η^5-Cp ring in **A**, **B**, **F**, **I**, and **J** that are pointing toward the boron atom, an effect described by Jemmis and Schleyer[27] in terms of the degree of overlap between the p orbitals of the boron atom with the e_1 orbitals of the Cp ring (see below).

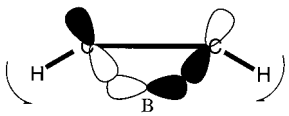

For **A** and **B**, the computed CH bending angles in the η^5-Cp ring are 9.9°, whereas those for **I** and **J** are 6.6° and 6.4°, respectively. The greater CH bending for **A** and **B** relative to **I** and **J** can be explained by the shorter B−C(π) distances in **A** and **B** and the corresponding greater the overlap between p-orbitals and e_1 orbitals of the Cp ring resulting in more inward bending of hydrogen atoms.

A schematic structural correlation for the ring exchange in the $[BCp_2]^+$ cation is given in Figure 3. The overall activation barrier is calculated to be 14.7 kcal/mol which is significantly greater than the activation barrier for ring exchange in beryllocene (<2 kcal/mol[6m−6o]). The larger activation barrier is due to the stronger interaction of the Cp rings with boron in borocenium than with beryllium in beryllocene as judged by the much shorter ring−ring separation in the D_{5d}-structures (3.040 and 3.325 Å, respectively). In a dynamic study of the

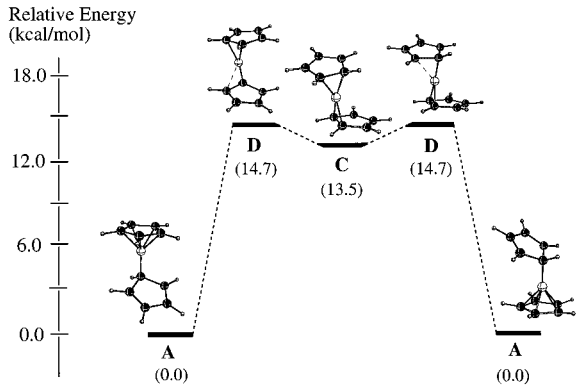

Figure 3. Schematic diagram for the ring exchange process of $[BCp_2]^+$ cation.

fluxional process in beryllocene,[6m−6o] the lowest-energy pathway involved η^2/η^5 and η^3/η^3 transition structures rather than the more symmetrical η^5/η^5 structure. In the ring exchange mechanism for borocenium, the lowest energy pathway also does not include a high-hapticity transition structure. Rather, the transition structure, **D**, is η^1/η^2 and leads to a shallow minimum (1.2 kcal/mol) for intermediate **C** which is of η^2/η^2 type. The exchange process reduces the hapticity of one Cp ring ($\eta^5 \rightarrow \eta^2 \rightarrow \eta^2 \rightarrow \eta^1 \rightarrow \eta^1$) while increasing the hapticity of the other Cp ring ($\eta^1 \rightarrow \eta^1 \rightarrow \eta^2 \rightarrow \eta^2 \rightarrow \eta^5$).

$[BCp^*_2]^+$ Structures. Optimized geometries from the ONIOM(B3LYP/6-31+G(d):HF/STO-3G) method are given in Figure 4 for decamethyl-substituted borocenium cation structures, while energies relative to **BB** are shown in Table 2 at various levels of theory. **BB**, the lowest-energy conformer, is an η^1/η^5 type C_s-symmetry structure with a staggered conformation which is consistent with the available crystal data.[8b] It is noted that the eclipsed η^1/η^5 $[BCp_2]^+$ cation is lower in energy than the staggered conformation, although the difference is small (0.1 kcal/mol). It is likely that the η^1/η^5 eclipsed conformation of $[BCp^*_2]^+$ may be destabilized by van der Waals repulsions between the methyl groups on the Cp* rings; this is supported by the fact that the B−C(σ) bond distance (1.596 Å) in **BB** (eclipsed) is longer than that of **B** (1.569 Å). The ONIOM-optimized geometry of **BB** is in excellent agreement with experiment as well as the full DFT-optimized geometry (**BB′**) as shown in Table 3. The shorter experimental B−C(σ) bond distance (1.583 Å)[8b] compared to the computed one (ONIOM,

TABLE 2: Relative Energies (kcal/mol) of $[BCp^*_2]^+$ at Various Theoretical Levels

species	P. G.	type	method-I[a]	method-II[b]	method-III[c]	method-IV[d]
AA	C_s	η^1/η^5	0.1	0.1	0.8	0.7
BB	C_s	η^1/η^5	0.0	0.0	0.0	0.0
CC	C_2	η^2/η^2	13.7	13.2	12.8	12.8
DD	C_1	η^1/η^2	16.0	15.1	14.4	
EE	C_{2h}	η^1/η^1	22.7	21.3	19.7	
FF	C_s	η^2/η^5	24.1	24.6	23.3	
GG	C_{2v}	η^1/η^1	36.3	33.9	33.3	
HH	C_{2v}	η^2/η^2	44.9	43.9	42.5	
II	D_{5d}	η^5/η^5	60.9	60.7	57.9	
JJ	D_{5h}	η^5/η^5	63.4	63.1	60.7	

[a] Method-I: ONIOM(B3LYP/6-31+G(d):HF/STO-3G). [b] Method-II: ONIOM(B3LYP/6-311+G(2d,p):HF/STO-3G)//ONIOM(B3LYP/6-31+G(d):HF/STO-3G). [c] Method-III: B3LYP/6-31+G(d)//ONIOM(B3LYP/6-31+G(d):HF/STO-3G). [d] Method-IV: B3LYP/6-31+G(d)//B3LYP/6-31+G(d).

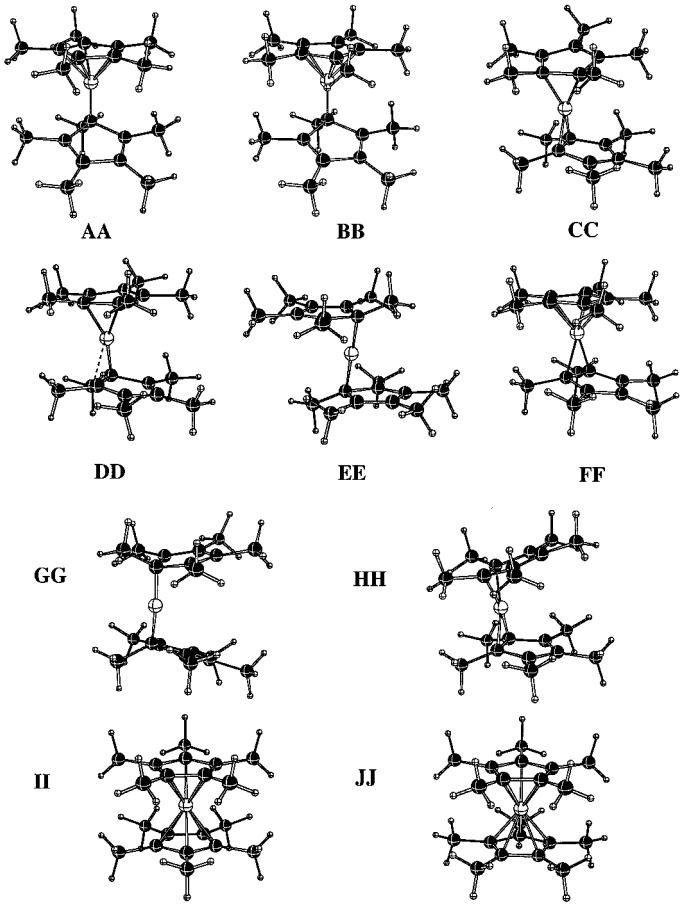

Figure 4. Optimized geometries of $[BCp^*_2]^+$ cations at ONIOM(B3LYP/6-31+G(d):HF/STO-3G) level.

TABLE 3: Calculated Geometrical Parameters of η^1/η^5 Conformer for $[BCp^*_2]^+$ at ONIOM(B3LYP/6-31+G(d):HF/STO-3G) and B3LYP/6-31+G(d) Levels[a]

parameters	**BB** (ONIOM)	**BB′** (DFT)	exptl. (staggered)[b]
r(B−C(σ))	1.596	1.595	1.583
r(B−C(π))	1.759 ∼ 1.783	1.765 ∼ 1.789	1.757 ∼ 1.782
∠(B−C(σ)-η^1−Cp*)	114.2	114.2	114.4

[a] Bond distance, Å; bond angle, degree. [b] Ref 8b.

TABLE 4: Calculated ^{11}B Chemical Shifts (ppm) at Various Theoretical Levels

species	NPA Boron charge[a] (Boron 2s density)	^{11}B GIAO Chemical Shifts B3LYP /6-31+G(d)	B3LYP /6-31+G(d,p)	B3LYP /6-311+G(d)	B3LYP /6-311+G(d,p)
A	0.93(0.56)	−47.9	−46.7	−50.7	−52.5
B	0.93(0.56)	−47.8	−46.6	−50.7	−52.4
C	0.78(0.58)	42.7	43.9	48.6	46.2
D	0.87(0.60)	14.0	15.2	16.8	14.7
E	1.02(0.64)	−5.2	−3.9	−2.7	−4.7
F	0.68(0.58)	−41.2	−40.0	−45.3	−47.3
G	1.31(0.70)	72.6	73.7	81.3	79.1
H	1.02(0.62)	55.5	56.8	60.7	58.1
I	0.60(0.55)	−61.0	−59.8	−69.5	−71.4
J	0.60(0.55)	−63.0	−61.2	−67.8	−69.8
BB[b]	0.83(0.54)	−42.4	−41.7	−46.8	−48.9
BB′[c]	0.83(0.54)	−42.4	−41.2	−46.5	−49.1

[a] From NBO analysis at B3LYP/6-31+G(d) level. Charge on boron is positive; 2s density in units of electrons. [b] On the basis of ONIOM(B3LYP/6-31+G(d):HF/STO-3G) optimized geometry. [c] On the basis of B3LYP/6-31+G(d) optimized geometry.

1.596 Å; DFT, 1.595 Å) could be due to crystal packing in the solid.

The relative energies of **AA**, **BB**, and **CC** are nearly identical between Method-III (geometries optimized with ONIOM) and Method-IV (geometries optimized at B3LYP/6-31+G(d); Table 2), whereas energy estimates from ONIOM methods (Method-I and Method-II) tend to somewhat overestimate steric repulsion (relative energies of **II** and **JJ** differ by about 3 kcal/mol). Overall, the relative energies among the $[BCp_2]^+$ and $[BCp^*_2]^+$ cations are very similar to each other, which suggests that Cp* metallocenes can be modeled by simpler Cp metallocenes. For example, the ring exchange process in **BB** → **DD(TS)** → **CC** → **DD(TS)** → **BB** has a calculated activation barrier of 14.4 kcal/mol,[28] very similar to the **A** → **C** → **A** process in the parent (14.7 kcal/mol).

The computed ^{11}B GIAO chemical shifts with various basis sets are presented in Table 4 along with the NPA charge and 2s electron density on boron for $[BCp_2]^+$ structures **A**−**J** and $[BCp^*_2]^+$ structures **BB** and **BB′**. The ^{11}B chemical shifts are moderately sensitive to basis set, especially the η^5/η^5 structures (**I** and **J**) where a 10 ppm change is found from 6-31+G(d) to 6-311+G(d,p). ^{11}B chemical shifts that are negative (**A**, **B**, **F**, **I**, and **J**) are moved further upfield with larger basis sets, whereas chemical shifts that are positive (**C**, **D**, **G**, and **H**) are moved further downfield. The span for ^{11}B chemical shifts of $[BCp_2]^+$ structures is remarkable, ranging from −61.2 to +73.7 ppm (**J** to **G**, GIAO/B3LYP/6-31+G(d,p)). The chemical shifts can be put into two groups; $[BCp_2]^+$ structures having at least one η^5 Cp ring have deshielded boron atoms (2s electron density less than 0.6 e$^-$) and upfield chemical shifts (−46.6 to −61.2 ppm; **A**, **B**, **F**, **I**, **J**). The second group has higher 2s electron densities and downfield shifts (+15.2 to +73.7 ppm; **D**, **G**, **H**). Structures **C** and **E** are exceptions, **C** having a small 2s electron density yet a downfield shift (+43.9 ppm), and **E** having a high 2s electron density and an upfield shift (−3.9 ppm).

Due to the inductive effect of alkyl substituent, the decamethyl-substituted Cp donates more electron density to vacant p_x and p_y orbitals of boron atoms relative to Cp (NPA positive charge on boron decreases from **B** (0.93) to **BB′** (0.83)) resulting in a 5.4 ppm downfield ^{11}B chemical shifts for $[BCp^*_2]^+$ relative to $[BCp_2]^+$ (GIAO/B3LYP/6-31+G(d,p)). The ^{11}B and ^{13}C chemical shifts of **B** and **BB′** calculated at the GIAO/B3LYP/6-31+G(d,p) level are compared with the experimental chemical shifts[8b] of decamethylborocenium in Table 5. The agreement is very good (the deviation in the ^{11}B chemical shifts is 0.3 ppm and the average deviation in ^{13}C chemical shifts is about 2 ppm) and fully supports the experimental assignments of the η^1/η^5 structure. The average ^{13}C chemical shift of the η^5 Cp ring carbons in **BB′** is 8.2 ppm downfield from the η^5 Cp ring carbons in **B**, whereas the η^1-Cp ipso-ring carbon in **BB′** is 18.3 ppm downfield from the corresponding carbon in **B**. Thus, whereas replacing a Cp* ring with a Cp ring has little effect on relative energies of different conformers, the effect on calculated ^{13}C chemical shifts is more significant.

TABLE 5: Calculated ^{11}B and ^{13}C Chemical Shifts (ppm) of BB′ and B at the GIAO/B3LYP/6-31+G(d,p)//B3LYP/6-31+G(d) Level

atom	**BB′** δ (calc)	**BB′** δ (exptl)	**B** δ (calc)
Boron	−41.2	−41.5	−46.6
η^5−CH_3	10.7	9.1	
η^5−Cp* ring C	110.6	112.9	102.4
η^1−Cp* ipso−CH_3	16.5	15.5	
η^1−Cp* ipso−ring C	47.8	51.8	29.5
η^1−Cp* α−CH_3	14.3	10.6	
η^1−Cp* α−ring C	135.4	136.4	131.2
η^1−Cp* β−CH_3	13.0	12.2	
η^1−Cp* β−ring C	141.7	138.1	135.7

Conclusions

The $[BCp_2]^+$ and $[BCp^*_2]^+$ cations were investigated at DFT and ONIOM levels where the lowest energy structure was found to be an η^1/η^5 type conformation, consistent with experiment. The energy difference between η^1/η^5 (**A**) and η^5/η^5 (**I**) structures of $[BCp_2]^+$ is 54.5 kcal/mol at the B3LYP/6-311+G(2d,p)//

B3LYP/6-31+G(d)+ZPC level. The high energy of the parallel sandwich structure (D_{5d}) may be due to the small size of boron atom resulting in greater repulsion between the Cp rings. Also contributing are the small size of p_x and p_y orbitals of boron which cannot effectively overlap with the e_1 orbitals of the Cp rings. The net effect is a preference of the η^1/η^5 structure (which satisfies the octet rule for boron) rather than an η^5/η^5 structure.

The ring exchange process for the $[BCp_2]^+$ cation, which has an activation energy barrier of 14.7 kcal/mol, undergoes a hapticity decrease of one ring ($\eta^5 \rightarrow \eta^2$(TS) $\rightarrow \eta^2 \rightarrow \eta^1$(TS) $\rightarrow \eta^1$) and a hapticity increases for the other Cp ring ($\eta^1 \rightarrow \eta^1$-(TS)$\rightarrow \eta^2 \rightarrow \eta^2$(TS) $\rightarrow \eta^5$). The symmetrical η^5/η^5 structure does not play a role in the ring exchange.

The lowest energy decamethylborocenium conformer is a staggered η^1/η^5 structure from both ONIOM and DFT methods. Comparison of geometrical parameters between experiment and theory are quite satisfactory. ^{11}B and ^{13}C chemical shift calculation are in excellent agreement with experiment. The methyl groups on the Cp rings are predicted to induce a 5.4 ppm downfield ^{11}B chemical shift, whereas the methyl group produced a 8.2 ppm downfield ^{13}C chemical shift of the η^5 carbons and a 18.3 ppm downfield ^{13}C chemical shift of the η^1 ipso-ring carbon.

Acknowledgment. Computer time was made available on the Alabama Supercomputer Network, the Maui High Performance Computer Center and the HP Exemplar at the University of Kentucky. An equipment grant from Sun Microsystems is acknowledged. We dedicate this paper to Prof. Younghi Kwon on the occasion of his retirement.

References and Notes

(1) (a) Wilkinson, G.; Roseblum, M.; Whiting, M. C.; Woodward, R. B. *J. Am. Chem. Soc.* **1952**, *74*, 2125. (b) *Ferrocenes*; Togni, A., Hayashi, T., Eds.; VCH: New York, 1995. (c) Laszlo, P.; Hoffmann, R. *Angew. Chem. Int. Ed.* **2000**, *39*, 123.

(2) For recent reviews, see: (a) Burkey, D. J.; Hanusa, T. P. *Comments Inorg. Chem.* **1995**, *17*, 41. (b) Beswick, M. A.; Palmer, J. S.; Wright, D. S. *Chem. Soc. Rev.* **1998**, *27*, 225. (c) Jutzi, P.; Burford, N. In *Metallocenes*; Togni, A., Halterman, R. L., Eds.; Wiley-VCH: New York, 1998; pp 3−54. (d) Long, N. J. *Metallocenes: An Introduction to Sandwich Complexes*; Blackwell Science: London, 1998. (e) Harder, S. *Coord. Chem. Rev.* **1998**, *176*, 17. (f) Jutzi, P.; Burford, N. *Chem. Rev.* **1999**, *99*, 969. (g) Kwon, O.; McKee, M. L. In *Computational Organometallic Chemistry*; Cundari, T. R., Ed.; Marcel Dekker: New York, 2001, pp 397−423.

(3) Wojtczak, W. A.; Fleig, P. F.; Hampden-Smith, M. J. *Adv. Organomet. Chem.* **1996**, *40*, 215.

(4) (a) Wong, C. H.; Lee, T. Y.; Chao, K. J.; Lee, S. *Acta Crystallogr. Sect. B* **1972**, *28*, 1662. (b) Wong, C. H.; Lee, T. Y.; Lee, T. J.; Chang, T. W.; Liu, C. S. *Inorg. Nucl. Chem. Lett.* **1973**, *9*, 667. (c) Nugent, K. W.; Beattie, J. K.; Hambley, T. W.; Snow, M. R. *Aust. J. Chem.* **1984**, *37*, 1601.

(5) Almenningen, A.; Haaland, A.; Lusztyk, J. *J. Organomet. Chem.* **1979**, *170*, 271.

(6) (a) Sundbom, M. *Acta Chem. Scand.* **1966**, *20*, 1608. (b) Haaland, A. *Acta Chem. Scand.* **1968**, *22*, 3030. (c) Lauher, J. W.; Hoffmann, R. *J. Am. Chem. Soc.* **1976**, *98*, 1729. (d) Marynick, D. S. *J. Am. Chem. Soc.* **1977**, *99*, 1436. (e) Collins, J. B.; Schleyer, P. v. R. *Inorg. Chem.* **1977**, *16*, 152. (f) Demuynck, J.; Rohmer, M. M. *Chem. Phys. Lett.* **1978**, *54*, 567. (g) Dewar, M. J. S.; Rzepa, H. S. *J. Am. Chem. Soc.* **1978**, *100*, 777. (h) Jemmis, E. D.; Alexandratos, S.; Schleyer, P. v. R.; Streitwieser, A., Jr.; Schaefer, H. F., III. *J. Am. Chem. Soc.* **1978**, *100*, 5695. (i) Gleiter, R.; Böhm, M. C.; Haaland, A.; Johansen, R.; Lusztyk, J. *J. Organomet. Chem.* **1979**, *170*, 285. (j) Glidewell, C. *J. Organomet. Chem.* **1981**, *217*, 273. (k) Gribov, L. A.; Raikhshtat, M. M.; Zhogina, V. V. *Koord. Khim.* **1988**, *14*, 1368. (l) Beattie, J. K.; Nugent, K. W. *Inorg. Chim. Acta* **1992**, *198*−*200*, 309. (m) Margl, P.; Schwarz, K.; Blöchl, P. E. *J. Am. Chem. Soc.* **1994**, *116*, 11 177. (n) Margl, P.; Schwarz, K.; Blöchl, P. E. *J. Chem. Phys.* **1995**, *103*, 683. (o) Schwarz, K.; Nusterer, E.; Margl, P.; Blöchl, P. E. *Int. J. Quantum Chem.* **1997**, *61*, 369. (p) Mire, L. W.; Wheeler, S. D.; Wagenseller, E.; Marynick, D. S. *Inorg. Chem.* **1998**, *37*, 3099.

(7) Wong, C.; Wang, S. *Inorg. Nucl. Chem. Lett.* **1975**, *11*, 677.

(8) (a) Jutzi, P.; Seufert, A. *J. Organomet. Chem.* **1978**, *161*, C5. (b) Voigt, A.; Filipponi, S.; Macdonald, C. L. B.; Gorden, J. D.; Cowley, A. H. *Chem. Commun.* **2000**, 911. (c) Macdonald, C. L. B.; Gorden, J. D.; Voigt, A.; Cowley, A. H. *Book of Abstracts*, 219th ACS National Meeting, San Francisco, CA.; American Chemical Society: Washington, DC, 2000; INOR-029.

(9) Dohmeier, C.; Schnöckel, H.; Robl, C.; Schneider, U.; Ahlrichs, R. *Angew. Chem., Int. Ed.* **1993**, *32*, 1655.

(10) Macdonald, C. L. B.; Gorden, J. D.; Voigt, A.; Cowley, A. H. *J. Am. Chem. Soc.* **2000**, *122*, 11 725.

(11) (a) Bochmann, M.; Dawson, D. M. *Angew. Chem., Int. Ed. Engl.* **1996**, *35*, 2226. (b) Heumann, L.; Richmond, T. G. *Chemtracts* **1998**, *11*, 893.

(12) (a) Parr, R. G.; Yang, W. *Density-Functional Theory of Atoms and Molecules*; Oxford University Press: Oxford, 1989. (b) Koch, W.; Holthausen, M. C. *A Chemist's Guide to Density Functional Theory*; Wiley & Sons: New York, 2000.

(13) Douglas, B.; McDaniel, D.; Alexander, J. *Concepts and Models of Inorganic Chemistry*; Wiley Publishers: New York, 1994.

(14) Froese, R. D. J.; Morokuma, K. In *Encyclopedia of Computational Chemistry*; Schleyer, P. v. R., Ed.; Wiley Publishers: New York, 1998; Vol. 2, pp 1244−1257.

(15) Frisch, M. J.; Trucks, G. W.; Schlegel, H. B.; Scuseria, G. E.; Robb, M. A.; Cheeseman, J. R.; Zakrzewski, V. G.; Montgomery, J. A., Jr.; Stratmann, R. E.; Burant, J. C.; Dapprich, S.; Millam, J. M.; Daniels, A. D.; Kudin, K. N.; Strain, M. C.; Farkas, O.; Tomasi, J.; Barone, V.; Cossi, M.; Cammi, R.; Mennucci, B.; Pomelli, C.; Adamo, C.; Clifford, S.; Ochterski, J.; Petersson, G. A.; Ayala, P. Y.; Cui, Q.; Morokuma, K.; Malick, D. K.; Rabuck, A. D.; Raghavachari, K.; Foresman, J. B.; Cioslowski, J.; Ortiz, J. V.; Stefanov, B. B.; Liu, G.; Liashenko, A.; Piskorz, P.; Komaromi, I.; Gomperts, R.; Martin, R. L.; Fox, D. J.; Keith, T.; Al-Laham, M. A.; Peng, C. Y.; Nanayakkara, A.; Gonzalez, C.; Challacombe, M.; Gill, P. M. W.; Johnson, B.; Chen, W.; Wong, M. W.; Andres, J. L.; Head-Gordon, M.; Replogle, E. S.; Pople, J. A. *Gaussian 98*, revision A.7; Gaussian, Inc.: Pittsburgh, PA, 1998.

(16) Becke, A. D. *J. Chem. Phys.* **1993**, *98*, 5648.

(17) (a) Svensson, M.; Humbel, S.; Froese, R. D. F.; Matsubara, T.; Sieber, S.; Morokuma, K. *J. Phys. Chem.* **1996**, *100*, 19 357. (b) Humbel, S.; Sieber, S.; Morokuma, K. *J. Chem. Phys.* **1996**, *105*, 1959. (c) Dapprich, S.; Komiromi, I.; Byun, K. S.; Morokuma, K.; Frisch, M. J. *THEOCHEM* **1999**, *461*−*462*, 1.

(18) (a) Froese, R. D. J.; Morokuma, K. *Chem. Phys. Lett.* **1999**, *305*, 419. (b) Vreven, T.; Morokuma, K. *J. Chem. Phys.* **1999**, *111*, 8799. (c) Remko, M.; Lyne, P. D.; Richards, W. G. *Phys. Chem. Chem. Phys.* **2000**, *2*, 2511. (d) Feldgus, S.; Landis, C. R. *J. Am. Chem. Soc.* **2000**, *122*, 12 714. (e) Vreven, T.; Morokuma, K. *J. Comput. Chem.* **2000**, *21*, 1419. (f) Remko, M.; Walsh, O. A.; Richards, W. G. *Phys. Chem. Chem. Phys.* **2001**, *3*, 901.

(19) The convention will be adopted of using a single boldface letter for $[BCp_2]^+$ conformation and double boldface letters for $[BCp^*_2]^+$. Thus, the **A** and **AA** conformation and symmetry of $[BCp_2]^+$ and $[BCp^*_2]^+$ will be the same.

(20) (a) Reed, A. E.; Weinstock, R. B.; Weinhold, F. *J. Chem. Phys.* **1985**, *83*, 735. (b) Reed, A.; Curtiss, L. A.; Weinhold, F. *Chem. Rev.* **1988**, *88*, 899. (c) Weinhold, F. A. In *Encyclopedia of Computational Chemistry*; Schleyer, P. v. R., Ed.; Wiley Publishers: New York, 1998; Vol. 3, pp 1792−1810.

(21) Wiberg, K. B. *Tetrahedron* **1968**, *24*, 1083.

(22) (a) Hameka, H. F. *Mol. Phys.* **1958**, *1*, 203. (b) Ditchfield, R. *Mol. Phys.* **1974**, *27*, 789. (c) Fleischer, U.; Wüllen, C. v.; Kutzelnigg, W. In *Encyclopedia of Computational Chemistry*; Schleyer, P. v. R., Ed.; Wiley Publishers: New York, 1998; Vol. 3, pp 1827−1835.

(23) Onak, T.; Landesman, H. L.; Williams, R. E.; Shapiro, I. *J. Phys. Chem.* **1959**, *63*, 1533.

(24) Kwon, O.; McKee, M. L. Unpublished results at the B3LYP/6-31+G(d) level.

(25) MOLDEN: Schaftenaar G.; Noordik, J. H. Molden: a pre- and post-processing program for molecular and electronic structures. *J. Comput.-Aided Mol. Design* **2000**, *14*, 123.

(26) Huheey, J. E.; Keiter E. A.; Keiter, R. L. *Inorg. Chem.*; Harper-Collins College Publishers: New York, 1993.

(27) Jemmis, E. D.; Schleyer, P. v. R. *J. Am. Chem. Soc.* **1982**, *104*, 4781.

(28) Vibrational frequencies, calculated at the ONIOM(B3LYP/6-31+G-(d):HF/STO-3G) level, indicate that **DD** is a transition structure.